

# Single ribosomal transcription units are linear, compacted Christmas trees in plant nucleoli

Pablo González-Melendi, Brian Wells, Alison F. Beven and Peter J. Shaw\*

Department of Cell Biology, John Innes Centre, Norwich Research Park, Colney, Norwich NR4 7UH, UK

Received 30 January 2001; revised 4 May 2001; accepted 16 May 2001.

\*For correspondence (fax +44 1603 450022; e-mail peter.shaw@bbsrc.ac.uk).

---

## Summary

The rDNA transcription units are enormous macromolecular structures located in the nucleolus and containing 50–100 RNA polymerases together with the nascent pre-rRNA attached to the rDNA. It has not previously been possible to visualize nucleolar transcription units directly in intact nucleoli, although highly spread preparations in the electron microscope have been imaged as 'Christmas trees' 2–3  $\mu\text{m}$  long. Here we determine the relative conformation of individual transcription units in *Pisum sativum* plant nucleoli using a novel labelling technique. Nascent transcripts were detected by a highly sensitive silver-enhanced 1 nm gold procedure, followed by 3D electron microscopy of entire nucleoli. Individual transcription units are seen as conical, elongated clusters approximately 300 nm in length and 130 nm in width at the thickest end. We further show that there were approximately 300 active ribosomal genes in the nucleoli examined. The underlying chromatin structure of the transcribing rDNA was directly visualized by applying a novel limited extraction procedure to fixed specimens in order to wash out the proteins and RNA, thus specifically revealing DNA strands after uranyl acetate staining. Using this technique, followed by post-embedding *in situ* hybridization, we observed that the nucleolar rDNA fibres are not extended but show a coiled, thread-like appearance. Our results show for the first time that native rDNA transcription units are linear, compacted Christmas trees.

**Keywords:** 1 nm immunogold, 3D electron microscopy, rDNA transcription units, BrUTP incorporation, plant nucleolus.

---

## Introduction

Gene transcription is carried out in eukaryotes by large, multi-subunit RNA polymerases, and is regulated by a complex series of transcription factors and other components. The cell's huge requirement for ribosomes is supported by a very high rate of production of ribosomal RNAs, which is achieved by having many tandem repeats of the rRNA genes and by loading each active gene with many copies of RNA polymerase I. Thus the rDNA transcription units, which are located in the nucleolus, are enormous macromolecular structures. Despite a great deal of structural analysis of nucleoli, we still have little idea of the native conformation or organization of the transcription units (Shaw and Jordan, 1995), although an understanding of their structural organization will be crucial in formulating hypotheses for transcriptional activity and regulation. The near-universal occurrence in eukaryotes of a nucleolus into which rDNA transcription is sequestered suggests that the detailed organization of

rDNA transcription is of great importance in achieving efficient ribosome biogenesis. Furthermore, the organization of nucleolar transcription by RNA polymerase I may provide a model for the organization of nucleoplasmic transcription by RNA polymerases II and III.

rDNA transcription units from amplified amphibian oocytes were spread out and visualized in the EM by Miller and Beatty (1969); see Miller and Bakken (1972) for a detailed technical description. These micrographs showed the path of the gene, spread to 2–3  $\mu\text{m}$  in length, with 50–100 engaged polymerase I complexes and nascent rRNA radiating away in a gradient of increasing length, the so-called 'Christmas trees'. Later, similar spread structures were observed from other species, including plants (Trendelenburg *et al.*, 1974). However, in the absence of any direct structural evidence, their native organization is still hotly debated. Scheer *et al.* (1997) visualized structures resembling Christmas trees in cavities within the

specialized nucleoli of grasshopper oocytes, but these structures have yet to be characterized in molecular terms. The only case in which any other transcription units have been visualized in a near-native conformation is the Balbiani ring 2 (BR2) of *Chironomus tentans*. However, these genes are transcribed by RNA polymerase II (Andersson *et al.*, 1980).

Short pulses of BrUTP incorporation were first introduced by Dundr and Raska (1993); Jackson *et al.* (1993); and Wansink *et al.* (1993) to map transcription sites. It has been shown that Br-RNA is not further processed (Dundr and Raska, 1993; Wansink *et al.*, 1994) and therefore BrUTP incorporation has become a widely used and reliable marker of nascent transcripts.

Previous work from our group using BrUTP incorporation and 3D confocal microscopy has shown that transcription is localized in many small foci throughout the dense fibrillar component (DFC) of the nucleolus in plants (Thompson *et al.*, 1997). A combination of BrUTP incorporation and *in situ* hybridization using probes to the 18S coding region and the non-transcribed spacer of the ribosomal repeat (NTS) showed that the nucleolar transcription foci contained the transcribed regions of a gene, but not the non-transcribed spacers (Thompson *et al.*, 1997). One interpretation of this observation is that each of the foci represents a single transcribed rDNA repeat, but the data could also be explained by other, more complex models involving more than one transcribed region looping into a single site, as has been suggested for mammalian nucleoli (Hozak *et al.*, 1994).

Although post-embedding immunogold EM techniques have been used to analyse the location of components of the nucleolar transcription complexes, including rDNA, rRNA and proteins (Hozak *et al.*, 1994; Mosgoeller *et al.*, 1998; Puvion-Dutilleul *et al.*, 1997; Scheer and Rose, 1984), this approach has not led to any direct interpretation of the organization of these structures in molecular terms. As only targets at the surface of the specimen are accessible to the labelling procedures, it is difficult to assign gold particles unambiguously to particular structures, as what is seen in the electron microscope is not the same as what is accessible. The intensity of labelling is low, as only a small fraction of the potential labelled targets are accessible.

To overcome these problems, 1 nm gold pre-embedding labelling and electron microscopy can be used. This approach, combining in-depth labelling with high-resolution microscopy, was first applied by Melcak *et al.* (1996) to map nucleolar transcription sites after BrUTP incorporation in onion root protoplasts.

Using BrUTP incorporation we have developed a novel 3D pre-embedding immunogold method applied to sections of tissue, which has given much greater sensitivity and higher labelling levels than has been achieved

previously. This high level of labelling clearly defined the size and shape of the individual transcription sites. Both from their characteristic elongated, conical shape, and from the differences in their thickness as a function of time of BrUTP incorporation, the transcription sites must represent individual transcribed rDNA genes, which are organized as linear, compacted Christmas trees.

## Results and discussion

### *Pre-embedding labelling method*

Conventional EM immunogold or *in situ* gold labelling is carried out on ultrathin sections after the tissue is embedded in resin. This provides good ultrastructural preservation, but only structures at the surface of the specimen are accessible to the labelling procedures. An alternative is to carry out labelling before embedding, and to use 1 nm gold probes which are sufficiently small to penetrate the tissue. However, even with 1 nm probes, a compromise between the penetration of the probes into the section and the structural preservation of the tissue had to be reached. Under our experimental conditions a high intensity of labelling, compatible with reasonable ultrastructural preservation, was achieved.

The method used in this paper is essentially the same as used for confocal microscopy, with some additional steps such as dehydration/rehydration in a methanol series and a mild digestion with pronase in order to improve the penetration of the gold probes across thick sections of tissue. Using a correlative approach, we have been able to visualize sections of the same nucleoli under both the confocal and the electron microscope, showing that the structure was well preserved at high resolution (Shaw *et al.*, 1995).

### *BrUTP labelling is seen as clusters of particles in the nucleolus*

Figure 1 shows serial EM sections through an entire nucleolus. A highly specific, intense BrUTP labelling is seen as extended, dense groups of silver-gold particles, localized in regions between the nucleolar vacuole and the nucleolar periphery, which correspond to the DFC (González-Melendi *et al.*, 2000). In some places the groups are connected to the extranucleolar condensed chromatin (arrows in Figure 1f,h). These regions of dense labelling are connected on consecutive sections as parts of meandering regions running through the nucleolus (Figure 1l). The silver-gold particles were often seen in elongated clusters 200–300 nm in length (Figure 2; Table 1). In different labelling experiments the number of particles per cluster varied from about 10–40. However, the number of particles per cluster within a given nucleolus

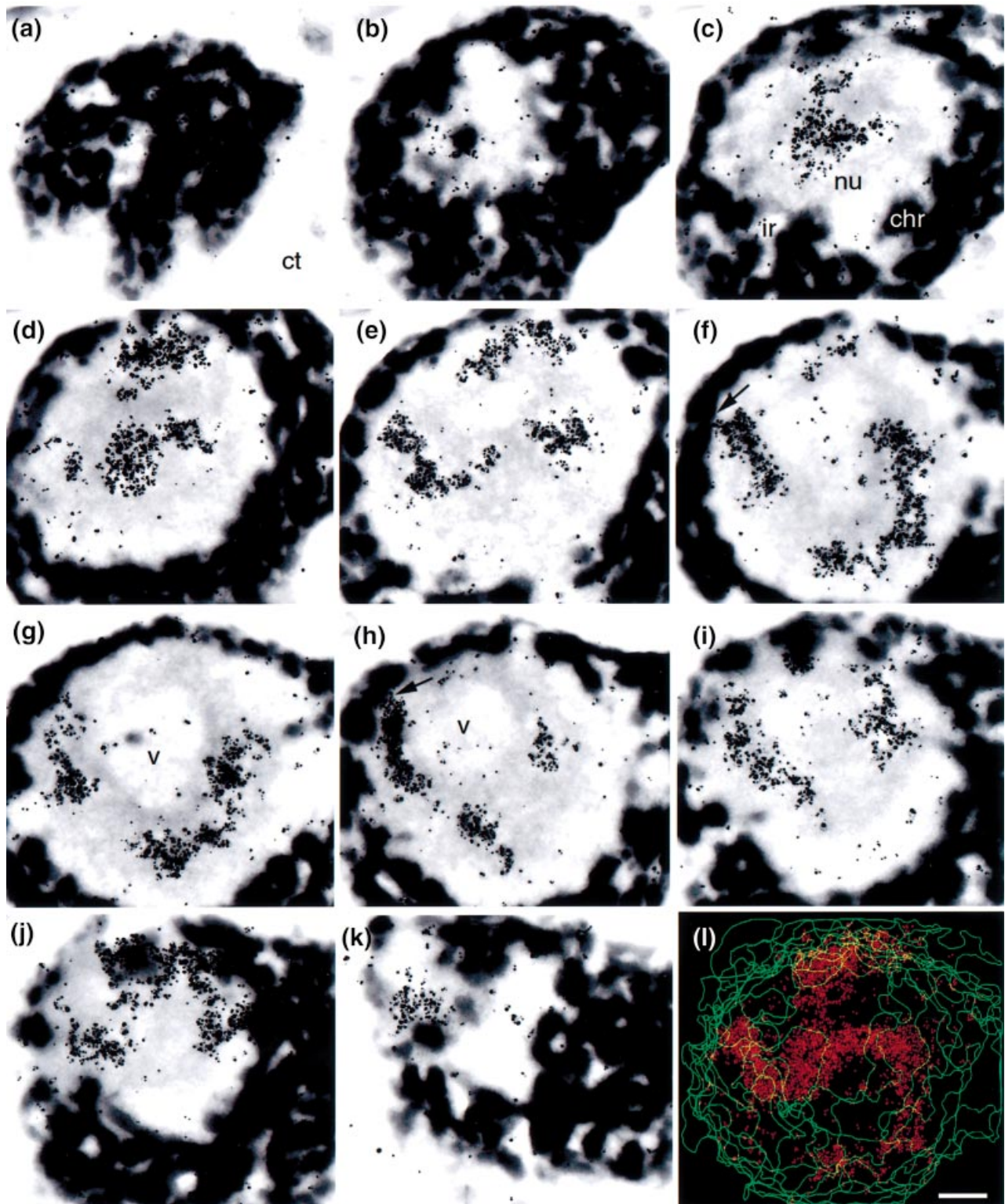


**Figure 1.** Detection of nucleolar transcription sites after 5 min incorporation of BrUTP and pre-embedding labelling in vibratome sections. (a–k) Series of 0.5  $\mu\text{m}$  EM sections through an entire nucleolus. The general nuclear morphology is well preserved. Labelling of rDNA transcription sites is seen as dark silver-gold particles within the nucleolar body (nu); there are also some particles in the interchromatin region (ir) at the periphery of the condensed chromatin (chr). Nucleolar transcription sites are localized in specific areas which, on some sections, are seen connected to the extranucleolar condensed chromatin (arrows) that presumably correspond to the knobs containing inactive rDNA genes. (l) 3D reconstruction of BrUTP labelling from serial sections. Each silver-gold particle is marked in red; the nucleolar outline is contoured in green. V, nucleolar vacuole. Scale bar, 1  $\mu\text{m}$ .

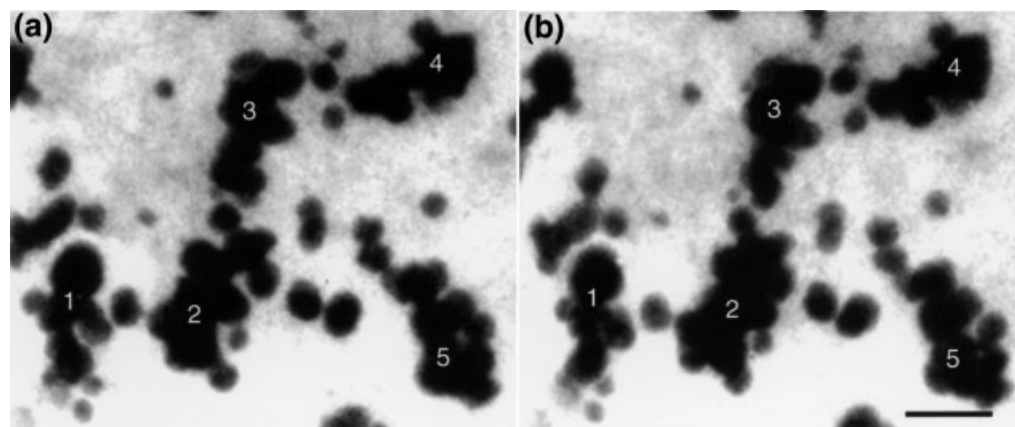


**Figure 2.** 3D visualization of individual transcription sites after 5 min BrUTP incorporation.

A stereo pair of a 0.5  $\mu\text{m}$  thick section was made by tilting the specimen  $+10^\circ$  and  $-10^\circ$ . In this area, five individual transcription sites are seen, the shortest about 200 nm long and 100 nm wide, and a gradient of thickness from one end to the other is seen along the clusters. Scale bar, 100 nm

was remarkably consistent, as shown by small standard deviations in particles per cluster (Table 2).

The density of particles per  $\mu\text{m}^3$  was calculated in the nucleolus and the cytoplasm; the latter was used as an estimate of the background (Table 3). The estimated background labelling, expressed as the ratio of the density of particles in the cytoplasm to the density in the nucleolus, ranged from 0.76 to 2% (Table 3). This very low background labelling consisted of isolated, single silver-gold particles, showing that there was no artefactual clustering of the label particles themselves.

#### *Each cluster corresponds to a single transcribed gene*

The simplest explanation is that each cluster corresponds to a single transcribed gene in the conformation of a compacted Christmas tree. To confirm this hypothesis, we carried out a time-course analysis. The estimated *in vivo* elongation rate of pre-rRNA is 1.1 kb  $\text{min}^{-1}$  (Karagyozyov *et al.*, 1980), and the length of the pea rDNA transcribed sequence is 6.6 kb (Jorgensen *et al.*, 1987; Thompson *et al.*, 1997). Thus, transcription of the primary pre-rRNA would be expected to take approximately 6 min. We therefore used incorporation times of 1 and 5 min. After 1 min, which would be expected to label about 10–20% of the length of the nascent transcripts, the clusters were thinner and somewhat shorter (Figure 3a–d) than after 5 min (Figure 3e–l). After 5 min incorporation, which should label most of the length of the transcripts, a gradient of thickness was observed from one end to the other of each cluster. Whereas the mean width at the thinner end was similar for both times ( $\approx 30$  nm), the width at the thicker end increased from approximately 50 nm after 1 min to 130 nm after 5 min (Table 1).

**Table 1.** Comparison of cluster size after 1 and 5 min BrUTP incorporation

	1 min BrUTP	5 min BrUTP
Mean length (nm)	213.47 $\pm$ 43.55	299.99 $\pm$ 60.71
Minimum length (nm)	142.85	214.28
Maximum length (nm)	357.14	464.28
Mean width, thin end (nm)	29.7 $\pm$ 7.49	30.35 $\pm$ 9.39
Mean width, thick end (nm)	54.55 $\pm$ 16.67	130.94 $\pm$ 43.33
Number of clusters examined	36	30

2D projections of the length and width of the thin and thick ends of clusters observed after 1 and 5 min BrUTP incorporation were measured on pictures from the same sets of experiments, to avoid misestimations due to a different progression of the silver-enhancing reaction. On average, clusters seen after 1 min BrUTP incorporation were 1.4 times shorter than those observed after 5 min, giving mean values of 213 and 299 nm, respectively. Whereas the mean width of the thin end was pretty similar in both cases, the width of the thick end was 2.4 times greater after 5 min incorporation.

These results strongly suggest that each cluster corresponds to a single rDNA transcription site in a linear conformation, as shown diagrammatically in Figure 4. After 1 min, the label on the nascent RNA is close to the axis of the gene (Figure 4a), whereas after 5 min the label would extend nearly to the end of the transcript (Figure 4b); this would be expected to give a higher level of labelling, and also a gradient of thickness of the cluster from one end to the other.

The predicted length of the complexes in Miller spreads in pea is 1.62  $\mu\text{m}$  (B-DNA has a length of 2.9 kb  $\mu\text{m}^{-1}$ , so 6.6 kb of B-DNA would be 2.27  $\mu\text{m}$  long, compacted by a ratio of about 1.4 in spreads; Scheer *et al.*, 1997). Thus the individual transcription units we have visualized, approximately 200–300 nm long, are compacted by

**Table 2.** Estimation of the number of nucleolar transcription complexes

	1 min BrUTP		5 min BrUTP		
	Nucleolus 1	Nucleolus 2	Nucleolus 3	Nucleolus 4	Nucleolus 5
Number of particles	2708	3540	5032	6328	10 825
Clusters counted	20	25	16	21	17
Particles/cluster	10.72 ± 1.85	12.04 ± 2.27	18.93 ± 2.75	22.71 ± 3.8	36.82 ± 4.8
Clusters/nucleolus	247	294	265	278	293

The number of transcription complexes per nucleolus was taken as the estimated number of BrUTP clusters. Five nucleoli were 3D-imaged from serial sections cut from pre-embedding labelled tissues after 1 min (nucleoli 1 and 2) and 5 min (nucleoli 3–5) of BrUTP incorporation. Total number of particles counted on each nucleolus. Single, well defined clusters were identified and the average number of particles per cluster was calculated for each model. The number of clusters per nucleolus was estimated by dividing the total number of particles per nucleolus by the average number of particles per cluster, giving an average number of  $275.4 \pm 17.76$  clusters per nucleolus.

**Table 3.** Estimation of background levels of BrUTP labelling

	1 min BrUTP		5 min BrUTP		
	Cell 1	Cell 2	Cell 3	Cell 4	Cell 5
Density P/V nucleolus ( $\mu\text{m}^{-3}$ )	59.68	80.45	99.15	229.09	324.10
Density P/V cytoplasm ( $\mu\text{m}^{-3}$ )	1.22	1.38	1.78	2.239	2.483
Estimate of background (%)	2	1.68	1.76	0.96	0.76

Background of BrUTP labelling was estimated on serial sections from pre-embedding labelled tissues after 1 (cells 1 and 2) and 5 min (cells 3–5) of BrUTP incorporation. On each section the nucleolar and cytoplasmic areas were estimated by counting the number of squares on a  $0.25 \mu\text{m}^2$  grid. Then the volumes were calculated by multiplying the area by the thickness of the section ( $0.5 \mu\text{m}$ ). The number of particles was counted on the nucleolus and the measured areas of the cytoplasm and the density of particles expressed in terms of volume. Background levels were expressed as the percentage of the density of particles in the cytoplasm in relation to total density per cell.

between 5 and 8 compared to Miller spreads. This interpretation of individual transcription units as foreshortened Christmas trees is in agreement with Scheer *et al.* (1997), who observed structures resembling Christmas trees approximately 400 nm in length within some nucleolar cavities in grasshopper oocytes, although these structures were not characterized in molecular terms. It is also consistent with the only case where transcription units have been unambiguously imaged by thin-section EM, the BR2 transcription units from the Balbiani rings of *C. tentans* (Andersson *et al.*, 1980). Although they are transcribed by RNA polymerase II rather than RNA polymerase I, the BR2 native transcription units are also linear Christmas trees (Andersson *et al.*, 1980; Daneholt *et al.*, 1982), in good agreement with our results.

Our interpretation of single rRNA genes as linear, compacted Christmas trees in plant nucleoli does not support current models for rDNA transcription in animal cells. Cook (1999) and Hozak *et al.* (1994) have suggested that up to four rRNA genes in an extended conformation are wound around fixed polymerases in a single fibrillar centre. They propose that during transcription the DNA would be pulled through the fixed polymerases around the

surface of the fibrillar centre as the nascent RNA is extruded into the surrounding DFC. Our results are not compatible with this model, and it has been shown that transcription sites in plants are not necessarily associated with fibrillar centres but are dispersed through the DFC (González-Melendi *et al.*, 2000; Melcak *et al.*, 1996; Thompson *et al.*, 1997).

#### *Number of active genes per nucleolus*

Complete series of  $0.5 \mu\text{m}$  sections from five similar nucleoli in the meristematic region of the roots were aligned and modelled in 3D using IMOD software (Kremer *et al.*, 1996). The nucleoli analysed corresponded to stages through S phase, as judged by structural features such as the number and size of nucleoli and presence of a nucleolar vacuole (Risueño and Medina, 1986). A number of individual, well defined clusters was identified in the 3D models and the original micrographs (approximately 20 clusters for each nucleolus), and the number of particles was counted in each cluster. Then the mean number of particles per cluster was calculated for each nucleolus (Table 2). The absolute labelling level varied about four-

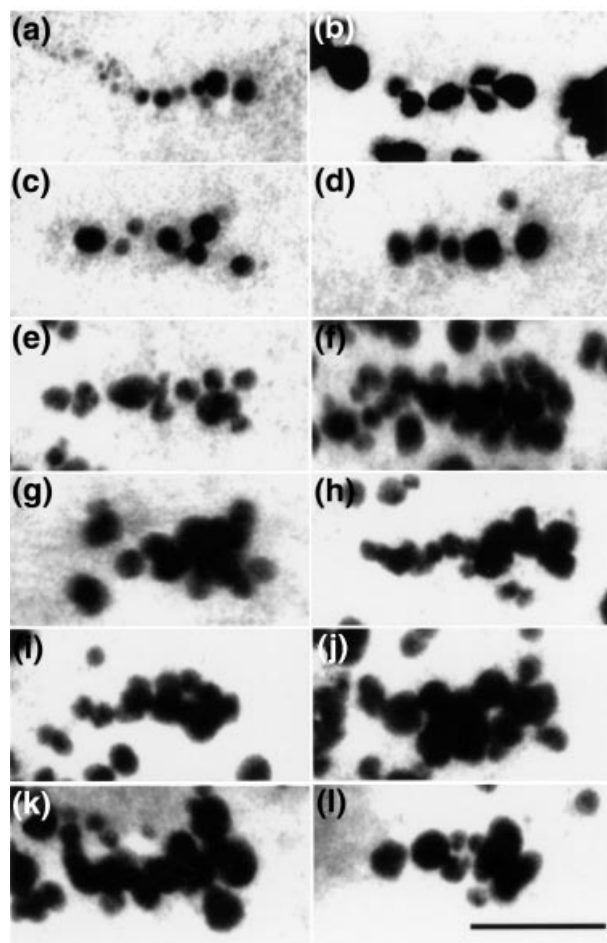


**Figure 3.** Gallery of single transcription units as seen after 1 (a–d) and 5 min (e–l) incorporation of BrUTP and pre-embedding labelling. 0.5  $\mu\text{m}$  thick sections. Labelling is seen as elongated clusters of particles whose length ranges from 200–300 nm. After 1 min BrUTP incorporation, the clusters appear thinner than after 5 min. After 5 min a gradient of thickness is seen from one end to the other of the clusters, suggesting compacted ‘Christmas trees’. Scale bar, 200 nm.

fold between different labelling experiments, and was significantly greater after 5 min incorporation. However, the number of particles per cluster was remarkably consistent within a given nucleolus. As each observed cluster corresponds to a single transcribed gene, the number of nucleolar transcription sites can be estimated, as in the serial section series we have imaged each entire nucleolus. Thus the number of transcription units per nucleolus was calculated by dividing the total number of particles in each nucleolus by the average number of particles per cluster for that nucleolus. This gave the number of transcription sites for each nucleolus, from 250 to 300, and was not dependent on the incorporation time (Table 2). This corresponds to less than 5% of the total number of rDNA genes in pea (Long and Dawid, 1980).

Comparable numbers of active rRNA genes have been reported for animal cells (Haaf *et al.*, 1991; Jackson *et al.*,

1993; Jackson *et al.*, 1998), although using more indirect methods. A study using antibodies to RNA polymerase I after 5,6-dichloro-1- $\beta$ -D-ribofuranosylbenzimidazole treatment, to unravel necklace-like structures within the nucleolus, estimated between 45 and 145 transcriptionally active rRNA genes in vertebrate cells, depending on the species (Haaf *et al.*, 1991). Using BrUTP incorporation into HeLa cells, Jackson *et al.* (1998) have determined the number of polymerases and estimated the number of transcription sites, finding  $\approx 15\,000$  polymerase I complexes and 120 active rRNA genes (Jackson *et al.*, 1998). Thus our calculations produced numbers of active genes similar to other estimates, further supporting the interpretation of the clusters as single genes.

#### *Direct visualization of nucleolar DNA*

In order to visualize directly the underlying chromatin structure of the transcribing rDNA, we developed a new ultrastructural staining technique for DNA. Although osmium ammine (Cogliati and Gautier, 1973; Derenzini *et al.*, 1982) and NAMA-Ur (Testillano *et al.*, 1991) have been used to reveal DNA specifically, the presence of highly packed proteins, some of them bound to the DNA, prevents access of the staining reagents to their targets, reducing sensitivity for detection of nucleolar DNA. Therefore we used a limited extraction procedure to wash out the proteins and RNA after specimen fixation. Vibratome sections of root tissue, fixed with a mixture of formaldehyde and glutaraldehyde, were treated with an extraction buffer containing SDS and proteinase K, then dehydrated and embedded in resin. Post-embedding *in situ* hybridization and 10 nm immunogold labelling on ultrathin sections, using probes to either the full ribosomal repeat or the NTS sequence, was then used to characterize the structures seen.

A complex network of threads was revealed within the nucleolus and the nucleolar area was surrounded by regions of condensed chromatin (Figure 5a). Most of the perinucleolar condensed chromatin was not labelled by the *in situ* gold probe (asterisks in Figure 5a,c), but some condensed chromatin masses were labelled (large arrows in Figure 5a,c); these must correspond to the perinucleolar knobs of condensed rDNA. The internal nucleolar network of fibres was extensively labelled, showing that the fibres correspond to or contain rDNA. The fibres had an intricate coiled appearance and were also often seen to emanate from the labelled perinucleolar masses of rDNA (Figure 5c). With the NTS probe, clusters of labelling were frequently seen at regular intervals, possibly reflecting sequential tandem repeats of the rDNA (Figure 5d).

These results support our model for the molecular organization of rRNA genes as foreshortened Christmas trees, showing that the nucleolar rDNA fibres are not

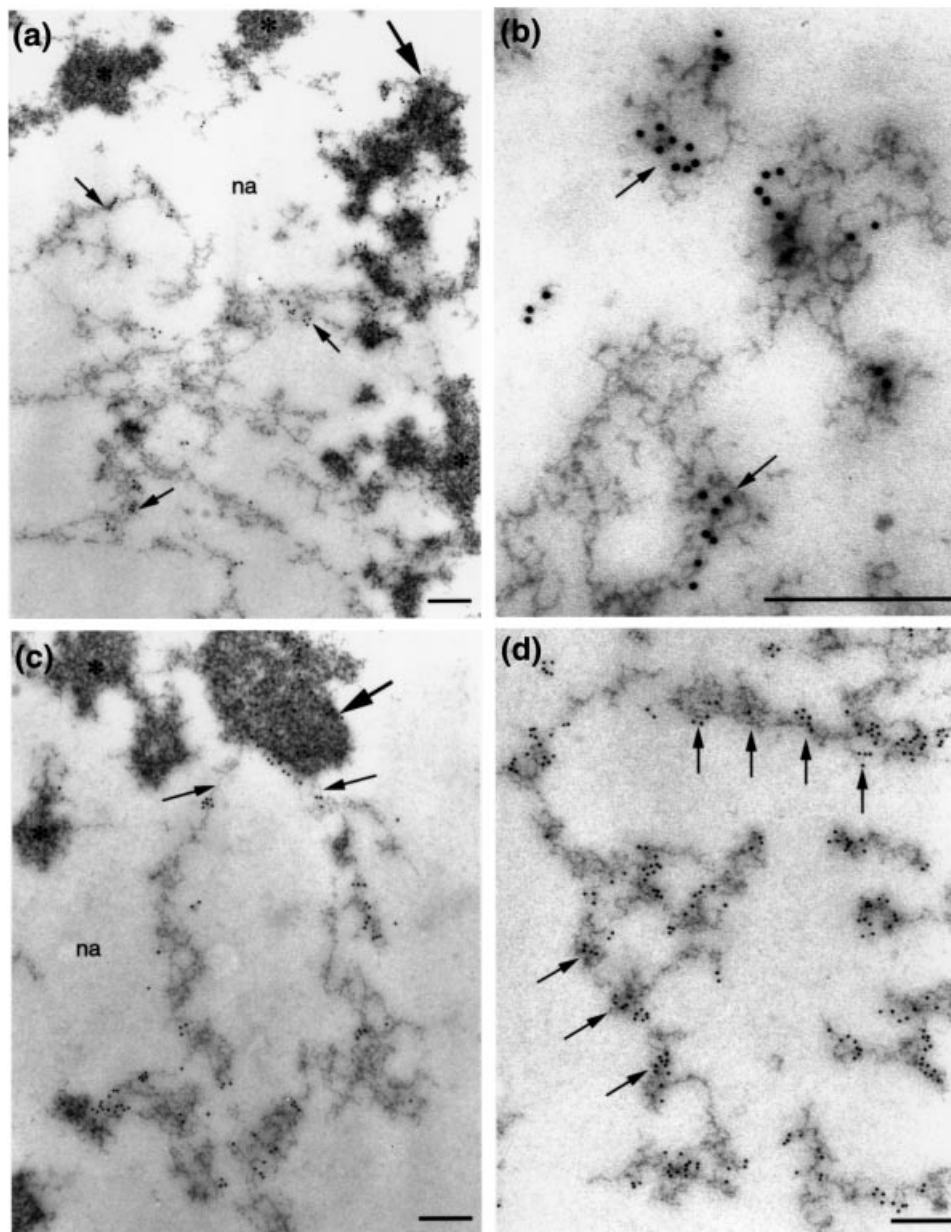


**Figure 5.** Ultrastructural visualization of nucleolar DNA combined with *in situ* hybridization on ultrathin sections using a probe to the rDNA repeat (a,b) and to the NTS sequence (c,d).

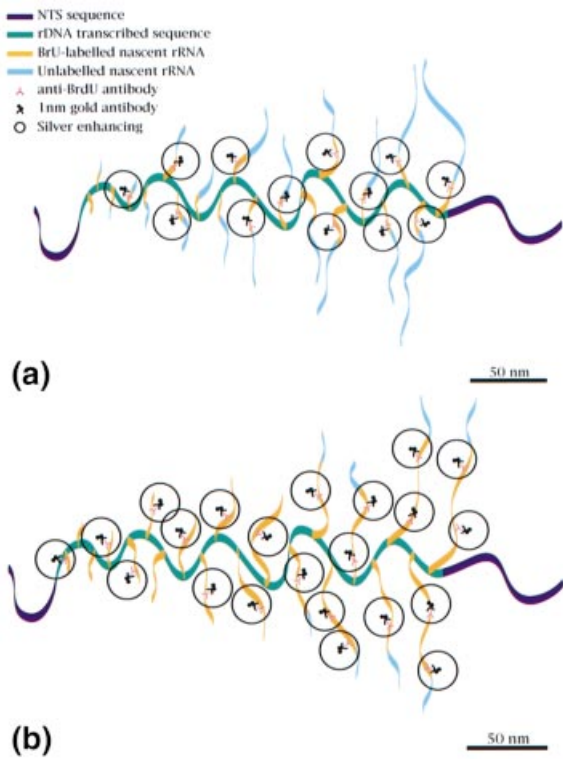
The nucleolar structure was disrupted to reveal a complex network of threads, and the nucleolar area was surrounded by regions of condensed chromatin (a) Most of the perinucleolar condensed chromatin was not labelled by the *in situ* gold probe (asterisks in a,c) but some condensed chromatin masses were labelled (large arrows in a,c); these must correspond to the perinucleolar knobs of condensed rDNA. The internal nucleolar network of fibres was extensively labelled, showing that the fibres correspond to or contain rDNA. The fibres had an intricate coiled appearance, and clusters of labelling were frequently seen at regular intervals, possibly reflecting sequential tandem repeats of the rDNA (d). Fibres were also often seen to emanate from the labelled perinucleolar masses of rDNA (c). Scale bar, 200 nm.

extended but have a coiled structure, consistent with significant compaction.

#### *Organization of rDNA transcription in plant nucleoli*

Figure 6 shows a working model for our interpretation of the nucleolar ultrastructure, in which the organization of tran-

scription is primarily determined by the arrangement of the rDNA in tandem repeats. The continuous thread of the rDNA is decondensed into meandering regions wherever the individual rDNA genes are transcriptionally active (a very small proportion of the total number of rDNA genes in this and most other plant species). Transcription units and intergenic spacers alternate in what is essentially a linear array.



Current models derived from studies in animal cells propose that the ribosomal genes are transcribed at the border between the fibrillar centres (FCs) and the DFC (Cook, 1999; Hozak *et al.*, 1994). In the present plant nucleoli and other cases, although in places several transcription units are grouped around a fibrillar centre, this is by no means always the case (González-Melendi *et al.*, 2000; Melcak *et al.*, 1996; Raska, 1995). Although the molecular processes of rDNA transcription and ribosome biogenesis are highly conserved between plants and animals, it is clear that the nucleolar ultrastructure seen in conventional thin-section EM is very different in these organisms. In many mammalian culture cells very clear FCs are surrounded by dense and compact regions of DFC. On the other hand, in typical plant nucleoli the DFC is

**Figure 4.** Molecular interpretation of BrUTP labelling, drawn approximately to scale. (a) At 1 min BrUTP incorporation, only 10–20% of the length of the transcripts is labelled, and particles detecting the nascent rRNAs are seen close to the gene. (b) At 5 min incorporation, most of the length of the transcripts is labelled by BrUTP and the silver-gold particles extend nearly to the end of the transcripts. This produces a gradient of the thickness of the clusters.

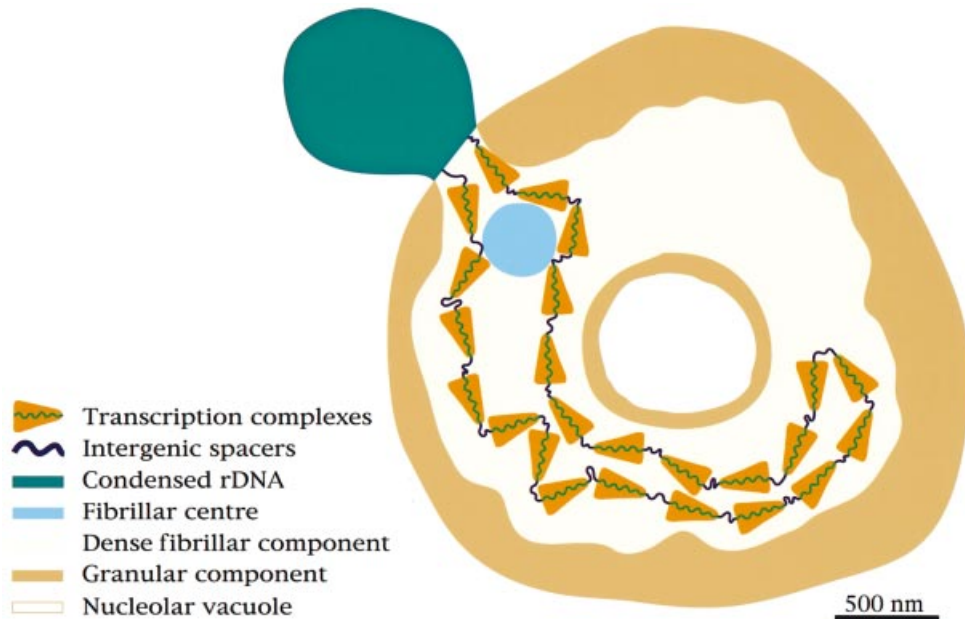


**Figure 6.** Interpretation of the nucleolar ultrastructure. Lined up five- to eightfold compacted ‘Christmas trees’ and intergenic spacers alternate on threads running through the dense fibrillar component (DFC), sometimes at the periphery of the FCs. This model suggests that the organization of nucleolar transcription is primarily determined by the arrangement of the rDNA in tandem repeats. For simplicity, only a single knob is shown, and only a few transcription units from the single NOR. In reality ≈300 transcription units from the four NORs are closely packed together, filling almost the whole DFC. Although only a single loop is shown originating from the NOR, our data cannot rule out the possibility that more than one loop originates from each NOR.

extensive and can occupy most of the nucleolar volume, and there is not usually a striking difference between the staining intensity of the granular component (GC) and the DFC (Shaw and Jordan, 1995). Furthermore, while in most animal species most of the rDNA may be active (typically a few hundred copies at most), in most plants there are far more copies (thousands) but only a small proportion can be active: about 5% in this study. However, the numbers of active genes inside the nucleolus in plants and animals are similar, and in plants the inactive genes are condensed into perinucleolar knobs. The reason for these differences is not known. Given the ultrastructural differences, it is perhaps not surprising that the organization of rDNA transcription in plants is different from that suggested by current models derived from studies of mammalian nucleoli. However, the level of detail we have revealed in these plant nucleoli is greater than has currently been achieved in animal nucleoli. A detailed comparison between the kingdoms must await a similar level of knowledge of animal nucleoli.

A minimal model for the generation of the observed nucleolar structure would simply be that a subset of rDNA genes becomes active, causing a segment of the chromosome to loop out from the NOR region of the chromosomes. Although there may be underlying structures such as FCs which organize the path of the active genes, it may not be necessary to invoke this as an organizing principle for the nucleolus. In our model, the DFC is simply the EM structure seen for hundreds of closely packed rDNA transcription units, each consisting of a compacted Christmas tree. The spaces between the transcription units must be filled with newly completed transcripts, in turn surrounded by preribosomal particles (Shaw *et al.*, 1995). The high degree of compactness of the overall structure, in which all available intranucleolar space is filled with nascent or detached RNP particles, must be the explanation for the difficulty of seeing the individual transcription units, unless, as in the present study, they are revealed by specific, visible labels; or, as was first done by Miller and colleagues, they are spread out.

## Experimental procedures

### Material

Seeds of *Pisum sativum* L. (pea) cv. Alaska were imbibed in aerated water for 12 h and germinated at 18°C for 2 days on water-soaked tissue paper.

### Preparation of probes

**RDNA probe.** Digoxigenin-labelled sense RNA probes to a single 8.8 kb rDNA repeat from pea (Jorgensen *et al.*, 1987) were synthesized by *in vitro* transcription, as previously described (Highett *et al.*, 1993).

**Non-transcribed spacer (NTS) probe.** Digoxigenin-labelled sense RNA probes to the 2.2 kb NTS from pea were synthesized by *in vitro* transcription as previously described (Thompson *et al.*, 1997). Probe size was reduced to approximately 100 bases by a mild carbonate hydrolysis (Cox *et al.*, 1984).

### BrUTP incorporation into tissue sections

The root tip containing the meristematic tissue was excised and 40 µm sections were cut using a vibratome (Vibratome series 1000, TAAB Laboratories Equipment Ltd, Aldermaston, UK) in modified physiological buffer (Hozak *et al.*, 1993; MPB: 100 mM potassium acetate; 20 mM KCl; 20 mM Hepes-KOH pH 7.4; 1 mM MgCl<sub>2</sub>; 1 mM ATP in 50 mM Tris pH 8; 1% v/v thiodiglycol; 2 mg ml<sup>-1</sup> aprotinin; 0.5 mM PMSF pH 7.4, with KOH containing 1 M 2-methyl-2,4-pentanediol). Tissue sections were transferred to a tissue-handling device (Wells, 1985) for subsequent ease of handling. BrUTP incorporation into the sections was performed as previously described (Thompson *et al.*, 1997), except that tissue permeabilization used 0.05% Tween 20 instead of Triton ×100 in MPB. The permeabilized tissue was incubated with the transcription mixture for either 1 or 5 min at room temperature. After the transcription reaction, sections were washed in MPB, fixed in a 4% formaldehyde solution (freshly made from paraformaldehyde) in PEM buffer (50 mM PIPES/KOH pH 6.9; 5 mM EGTA; 5 mM MgSO<sub>4</sub> pH 7.4) for 1 h at room temperature and washed in PBS (140 mM NaCl; 3 mM KCl; 4 mM Na<sub>2</sub>HPO<sub>4</sub>; 2 mM KH<sub>2</sub>PO<sub>4</sub> pH 7.4) and water. Then the sections were dried on multiwell slides, coated with glutaraldehyde-activated 3-aminopropyl triethoxy silane (APTES) to ensure that the sections remained attached to them throughout the subsequent manipulations. BrUTP incorporation sites were detected by 1 nm pre-embedding immunogold labelling. To improve the penetration of the gold probes into the tissues, the sections were treated as follows: dehydration and rehydration through a methanol series (Melcak *et al.*, 1996), 2% cellulase (Onozuka R-10) in PBS for 1 h at room temperature, 0.125 mg ml<sup>-1</sup> pronase (Sigma Aldrich Company Ltd, Poole, Dorset, UK) in reaction buffer (1 mM Tris pH 7.8; 1 mM EDTA; 0.5% SDS) for 15 min at 37°C and 0.1% Tween 20 in PBS for 10 min. In control experiments the processing was carried out without dehydration and gave the same labelling patterns, but with lower levels of labelling.

### Pre-embedding immunogold labelling

Sections were treated with 3% BSA in PBS for 10 min followed by incubation for 90 min at room temperature with mouse anti-BrdU antibodies (Boehringer Mannheim GmbH, Mannheim, Germany) applied 1/20 in PBS. Then a secondary anti-mouse 1 nm gold antibody (BioCell Research Labs, Cardiff, UK) was applied 1/100 in PBS overnight at 4°C. After extensive washes in PBS and water, the gold particles were amplified using a silver-enhancing kit (BioCell). The reaction was monitored under an inverted light microscope. When a faint signal was detected, silver enhancing was stopped in water. Then the sections were post-fixed with 1% glutaraldehyde in PBS for 15 min, and washed before processing for electron microscopy. In control experiments omitting either the primary or secondary antibody or the silver enhancement, no silver-gold particles were seen.

### Ultrastructural visualization of nucleolar DNA

Root tips were fixed in a 4% formaldehyde and 0.1% glutaraldehyde solution in PEM for 1 h at room temperature. After washing

in PBS, 40 µm vibratome sections were cut under water and dried down on APTES-coated multiwell slides, then permeabilized by dehydration and subsequent rehydration through a methanol series and a 2% cellulase treatment for 1 h at room temperature. Sections were incubated with a DNA extraction buffer containing 100 mM Tris pH 8.0, 100 mM NaCl, 50 mM EDTA, 2% SDS and 0.05 mg ml<sup>-1</sup> proteinase K for 45 min at 37°C, washed, and stored in PBS overnight at 4°C. They were then processed for electron microscopy.

#### Specimen processing and electron microscopy

Sections on multiwell slides were dehydrated through an ethanol series and infiltrated in LR white resin (Agar Scientific Ltd, Stanstead, Essex, UK) containing 0.5% benzoin methyl ether as catalyst, in a series 1 : 1, 1 : 2, 1 : 3 ethanol : resin, and finally 100% resin overnight at -20°C. Slides containing sections were taken out of the resin, and a gelatin capsule filled with resin containing the catalyst was inverted over each well. The resin was allowed to polymerize at room temperature overnight under UV light. The polymerized blocks were detached from the slide by cooling in liquid nitrogen.

Sections ranging from 100 nm to 1 µm were cut using a Leica Ultracut E and collected on 200-mesh grids coated with pyroxylin. Series of 0.5 µm thick sections were collected on slot grids coated with formvar. Sections were stained with 2% (w/v) aqueous uranyl acetate for 40 min. Electron microscopy was carried out with a Jeol 1200 EX electron microscope running at either 80 or 120 kV depending on the thickness of the sections. The specimen holder was mounted on a eucentric goniometer stage that permitted grid tilting from -60° to +60° for recording tilted views.

#### In situ hybridization on ultrathin sections

Detection of rDNA sequences on ultrathin sections was performed according to Puvion-Dutilleul and Puvion (1996). Gold grids carrying the sections were incubated for 2 h at 37°C in a humid chamber with the hybridization mixture containing ≈200 ng µl<sup>-1</sup> digoxigenin-labelled probe; ≈1000 ng µl<sup>-1</sup> unlabelled RNA transcribed from a plasmid containing an unrelated insert; 50% deionized formamide; 10% dextran sulfate; 300 mM NaCl; 10 mM PIPES pH 8.0; 1 mM EDTA. After washing in PBS, the hybridization signal was detected by a primary mouse anti-digoxigenin antibody (Sigma) and a secondary anti-mouse 10 nm gold antibody (BioCell) applied 1/5000 in 3% BSA in PBS and 1/25 in PBS, respectively, for 1 h at room temperature. Finally, sections were stained with 2% (w/v) aqueous uranyl acetate for 40 min.

#### 3D modelling of nucleolar transcription sites

Serial sections from pre-embedding labelled tissues were used for computer-assisted 3D modelling of nucleolar transcription sites. Micrographs of consecutive 0.5 µm sections across entire nucleoli were photocopied on transparencies for pairwise manual alignment on a light box. Then the original micrographs were trimmed down and scanned at 300 dpi [SCANMAKER 5, Microtek (sales@microtek.com)]. 3D reconstructions were modelled using a Silicon Graphics computer running the IMOD software (Kremer et al., 1996). On each section the outline of the nucleolus was contoured and each silver-gold particle was marked as a point. The nucleolar contours and the particles were considered as distinct objects and a different colour was assigned to each one.

#### Estimation of the number of transcription sites

Individual and well defined clusters of particles were selected on original micrographs. They were then identified on the 3D models and the number of particles counted on each one. The number of clusters per nucleolus was estimated by dividing the total number of particles per nucleolus by the mean number of particles per cluster.

#### Preparation of figures

3D models from IMOD were saved in Silicon Graphics format, then made into final figures on a Macintosh computer using PHOTOSHOP (Adobe Systems Inc., Mountain View, CA, USA). Diagrams were drawn using ILLUSTRATOR (Adobe). Pictures were printed on a Pictography P3000 printer (Fujix).

#### Acknowledgements

We thank Dr Gwyn Jordan and Dr Liam Dolan for advice and discussion, Dr David Mastrorade at the Boulder Laboratory for 3D Fine Structure, University of Colorado for generously providing the IMOD program, and for help in its use, and Sue Bunnewell for expert photographic work. This work was supported by the Biotechnology and Biological Sciences Research Council of the UK.

#### References

- Andersson, K., Björkoth, B. and Daneholt, B. (1980) The *in situ* structure of the active 75S RNA genes in Balbiani rings of *Chironomus tentans*. *Exp. Cell Res.* **130**, 313–326.
- Cogliati, R. and Gautier, A. (1973) Mise en évidence de l'and et des polysaccharides à l'aide d'un nouveau réactif 'de type Schiff'. *CR Acad. Sci.* **276**, 3041.
- Cook, P.R. (1999) The organisation of replication and transcription. *Science*, **284**, 1790–1795.
- Cox, K.H., DeLeon, D.V., Angerer, L.M. and Angerer, R.C. (1984) Detection of mRNAs in sea urchin embryos by *in situ* hybridization using asymmetric RNA probes. *Dev. Biol.* **50**, 353–359.
- Daneholt, B., Anderson, K., Björkoth, B. and Lamb, M.M. (1982) Visualization of active 75S RNA genes in the Balbiani rings of *Chironomus tentans*. *Eur. J. Cell Biol.* **26**, 325–332.
- Derenzini, M., Viron, A. and Puvion-Dutilleul, F. (1982) The Fuelgen-like osmium-ammine reaction as a tool to investigate chromatin structure in thin sections. *J. Ultrastruct. Res.* **80**, 133.
- Dundr, M. and Raska, I. (1993) Nonisotopic ultrastructural mapping of transcription sites within the nucleolus. *Exp. Cell Res.* **208**, 275–281.
- González-Melendi, P., Beven, A., Boudonck, K., Abranches, R., Wells, B., Dolan, L. and Shaw, P. (2000) The nucleus: a highly organized but dynamic structure. *J. Microsc.* **198**, 199–207.
- Haaf, T., Hayman, D.L. and Schmid, M. (1991) Quantitative determination of rDNA transcription units in vertebrate cells. *Exp. Cell Res.* **193**, 78–86.
- Highett, M.I., Rawlins, D.J. and Shaw, P.J. (1993) Different patterns of rDNA distribution in *Pisum sativum* nucleoli correlate with different levels of nucleolar activity. *J. Cell Sci.* **104**, 843–852.
- Hozak, P., Hassan, A.B., Jackson, D.A. and Cook, P.R. (1993) Visualization of replication factories attached to a nucleoskeleton. *Cell*, **73**, 361–373.

- Hozak, P., Cook, P.R., Schöfer, C., Mosgöller, W. and Wachtler, F.** (1994) Site of transcription of ribosomal RNA and intranucleolar structure in HeLa cells. *J. Cell Sci.* **107**, 639–648.
- Jackson, D.A., Hassan, A.B., Errington, R.J. and Cook, P.R.** (1993) Visualization of focal sites of transcription within human nuclei. *EMBO J.* **12**, 1059–1065.
- Jackson, D.A., Iborra, F.J., Manders, E.M.M. and Cook, P.R.** (1998) Numbers and organisation of RNA polymerases, nascent transcripts and transcription units in HeLa nuclei. *Mol. Biol. Cell.* **9**, 1523–1536.
- Jorgensen, R.A., Cuellar, R.E., Thompson, W.F. and Kavanagh, T.A.** (1987) Structure and variation in ribosomal RNA genes of pea. *Plant Mol. Biol.* **8**, 3–12.
- Karagyozov, L.K., Stoyanova, B.B. and Hadjiolov, A.A.** (1980) Effect of cycloheximide on the *in vivo* and *in vitro* synthesis of ribosomal RNA in rat liver. *Biochim. Biophys. Acta.* **607**, 295–303.
- Kremer, J.R., Mastronarde, D.N. and McIntosh, J.R.** (1996) Computer visualization of three-dimensional image data using IMOD. *J. Struct. Biol.* **116**, 71–76.
- Long, E.O. and Dawid, B.** (1980) Repeated genes in eukaryotes. *Ann. Rev. Biochem.* **49**, 727–764.
- Melcak, I., Risueño, M.C. and Raska, I.** (1996) Ultrastructural nonisotopic mapping of nucleolar transcription sites in onion protoplasts. *J. Struct. Biol.* **116**, 253–263.
- Miller, O.L. and Bakken, A.H.** (1972) Morphological studies on transcription. *Acta Endocrinol. Suppl.* **168**, 155–177.
- Miller, O.L. and Beatty, B.R.** (1969) Visualization of nucleolar genes. *Science*, **164**, 955–957.
- Mosgoeller, W., Schöfer, C., Wesierska-Gadek, J., Steiner, M., Müller, M. and Wachler, F.** (1998) Ribosomal gene transcription is organized in foci within nucleolar components. *Histochem. Cell Biol.* **109**, 111–118.
- Puvion-Dutilleul, F. and Puvion, E.** (1996) Non-isotopic electron microscope *in situ* hybridization for studying the functional sub-compartmentalization of the cell nucleus. *Histochem. Cell Biol.* **106**, 59–78.
- Puvion-Dutilleul, F., Puvion, E. and Bachellerie, J.-P.** (1997) Early stages of pre-rRNA formation within the nucleolar ultrastructure of mouse cells studied by *in situ* hybridization with a 5' ETS leader probe. *Chromosoma*, **105**, 496–505.
- Raska, I.** (1995) Nuclear ultrastructures associated with the RNA synthesis and processing. *J. Cell. Biochem.* **59**, 11–26.
- Risueño, M.C. and Medina, F.J.** (1986) The nucleolar structure in plant cells. *Cell Biol. Rev.* **7**, 1–143.
- Scheer, U. and Rose, K.M.** (1984) Localization of RNA polymerase I in interphase cells and mitotic chromosomes by light and electron microscopic immunocytochemistry. *Proc. Natl Acad. Sci. USA*, **81**, 1431–1435.
- Scheer, U., Xia, B., Merkert, H. and Weisenberger, D.** (1997) Looking at Christmas trees in the nucleolus. *Chromosoma*, **105**, 470–480.
- Shaw, P.J. and Jordan, E.G.** (1995) The nucleolus. *Annu. Rev. Cell Dev. Biol.* **11**, 93–121.
- Shaw, P.J., Highett, M.I., Beven, A. and Jordan, E.G.** (1995) The nucleolar architecture of polymerase I transcription and processing. *EMBO J.* **14**, 2896–2906.
- Testillano, P.S., Sanchez-Pina, M.A., Olmedilla, A., Ollacizqueta, M.A., Tandler, C.J. and Risueño, M.C.** (1991) A specific ultrastructural method to reveal DNA: the NAMA-Ur. *J. Histochem. Cytochem.* **39**, 1427–1438.
- Thompson, W.F., Beven, A.F., Wells, B. and Shaw, P.J.** (1997) Sites of rDNA transcription are widely dispersed through the nucleolus in *Pisum sativum* and can comprise single genes. *Plant J.* **12**, 571–581.
- Trendelenburg, M.F., Spring, H., Scheer, U. and Franke, W.W.** (1974) Morphology of nucleolar cistrons in a plant cells, *Acetabularia mediterranea*. *Proc. Natl Acad. Sci. USA*, **71**, 3626–3630.
- Wansink, D.G., Schul, W., Van der Kraan, I., Van Steensel, B., Van Driel, R. and De Jong, L.** (1993) Fluorescent labelling of nascent RNA reveals transcription by RNA polymerase II in domains scattered throughout the nucleus. *J. Cell Biol.* **112**, 283–293.
- Wansink, D.G., Nelissen, R.L. and De Jong, L.** (1994) *In vitro* splicing of pre-mRNA containing bromouridine. *Mol. Biol. Rep.* **19**, 109–113.
- Wells, B.** (1985) Low temperature box and tissue handling device for embedding biological tissue for immunostaining in electron microscopy. *Micron. Microsc. Acta*, **16**, 49–53.